Dust climatology from NOMAD UVIS channel

Z. Flimon[1], J. Erwin[1], A.C. Vandaele[1], L. Neary[1], A. Piccialli[1], L. Trompet[1], Y. Willame[1], F. Daerden[1], S. Bauduin[2], I. R. Thomas[1], B. Ristic[1], J. Mason[3], C. Depiesse[1], M. R. Patel[3], G. Bellucci[4], J.-J. Lopez-Moreno[5]

[1] **Royal Belgian Institute for Space Aeronomy, BIRA-IASB**
[2] **Université libre de Bruxelles (ULB), Spectroscopy, Quantum Chemistry and Atmospheric Remote Sensing (SQUARES), Brussels, Belgium**
[3] **School of Physical Sciences, The Open University, Milton Keynes, UK**
[4] **Instituto de Astrofisica e Planetologia Spaziali, INAF, Rome, Italy**
[5] **Instituto de Astrofisica de Andalucía, Consejo Superior de Investigaciones Científicas (CSIC), Granada, Spain**

Introduction:

Aerosols present in the atmosphere of Mars have a major effect on it. They are mainly composed of dust, water ice or CO_2 ice. Dust is confined to lower altitudes during the aphelion season and can reach higher altitudes during the perihelion, especially during dust storms that frequently arise on Mars. These storms can sometime grow up to cover the entire planet and are then called a global dust storm.
Notable observed water ice cloud features include polar hood and the Aphelion cloud belt (Clancy et al., 1996); CO_2 ice clouds can be observed seasonally at high altitudes (Montmessin et al., 2006),(Liuzzi et al., 2021). Where water ice clouds can be found mainly during perihelion and CO_2 cloud during aphelion. Dust can be found all the year round at low altitude and represent the main component of Martian aerosols.

As explained before dust can be transported to high altitudes during perihelion and dust storms. Dust in the atmosphere can have different effects, for example during dust storms it can be responsible for hydrogen loss (Holmes et al., 2021). Also, one of the most important effects of dust is the local atmospheric warming: the sun heats the dust which then heat up the local atmosphere. Knowing the vertical profile of dust is important to know the temperature profile.

Aerosols climatology has been studied by previous missions in solar occultation with SPICAM on board Mars Express (Määttänen et al., 2013), (Fedorova et al., 2014) or with limb measurement with CRISM. (Clancy et al., 2019). In this work we will focus our analysis on the UVIS channel of NOMAD.

The NOMAD ("Nadir and Occultation for MArs Discovery") spectrometer suite on board the ExoMars Trace Gas Orbiter (TGO) is composed of three spectrometers, two in IR (LNO and SO) and one in UV-visible (UVIS).

The UVIS spectral range extends from 200nm to 650nm with a spectral resolution about 1.5nm. UVIS can operate in nadir and occultation modes. In this work, we use observations taken in occultation mode to investigate the vertical distribution of aerosols. The altitude resolution of UVIS is below 300m and the SNR greater than 1000 for wavelength between 230-450nm, and generally larger than 500 for wavelength between 450-650nm (Vandaele et al., 2015). Using the UVIS channel, this work will permit to have a great precision when studying the vertical profile of aerosols and also spectral features.

We analyzed data from 2018 to 2021 covering 2 Martian years (see figure 1).
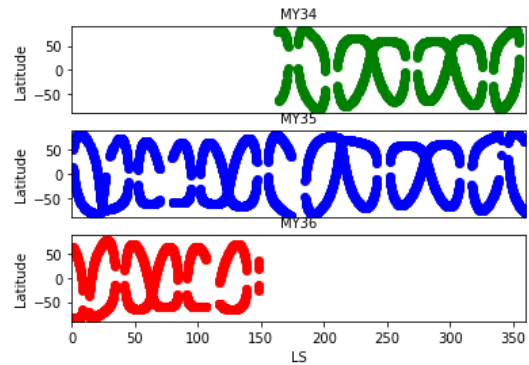

Figure 1 : Repartition of UVIS solar occultation between Martian years 34 to 36

We cover practically all the latitudes, this will give us the data necessary to build a complete climatology of aerosols in the Martian atmosphere.

Method:

To compute aerosol's extinction, from the transmittances of UVIS. We use first the ASIMUT code (Vandaele, et al., 2006.) to make a fit on ozone and Rayleigh scattering and then subtract them from the original transmittances. In the result should remain only the background of the spectra. Extinction can be computed from the transmittance after subtraction of ASIMUT's fit using the formula from (Wilquet et al., 2012):

$$\tau = -ln(T) = ln(I/I_0)$$
$$\beta_n(\lambda) = \frac{\tau - \sum_{i=1}^{N-1} dz\beta_i(\lambda,z)}{dz_n}$$

With τ the optical depth , T the transmittance, I the solar irradiance attenuated through the atmosphere and I_0 the reference irradiance of the solar spectrum

outside the atmopshere. β represents the extinction and N the number of layer above the current layer n. λ represents the wavelength and dZ represents the pathlength of light through the atmosphere to the point and i represent the upper layer.

To confirm the validity of our observations, only the data with a SNR > 8 and a minimum of 100 points in the spectra are kept.

The extinction is fitted using the refractive index for Mars dust from (Wolff et al., 2009). The extinction efficiency, Q_{ext} is computed using a Mie code (Bohren, et al., 1998) with a log normal size distribution, exploring the parameter space of effective radius (R_{eff}) from 0.1 to 2 micron, and standard deviation (V_{eff}) of 0.01 to 0.3 micron.

Given the Q_{ext} for each size distribution, the number density "n" is fitted using the relation $\beta = n * Q_{ext}$, with β the extinction derived from the UVIS spectra. The fit is made for each effective radius and each standard deviation. The best fit finally selected will be the one with the smallest reduced chi square.

The number density error is calcultated based on the extinction error with a Monte Carlo algorithm.

Results:

Using only the spectral range of UVIS, the dust, water ice and CO_2 ice cannot be differentiated because the three aerosols have similar spectral features in the UV-visible. However, it is possible to distinguish the particle size. Therefore, only dust will be assumed in this work. Detection of CO_2 and water ice will be investigated in a future work

We observe three different spectral features characteristic of dust in the UV. Large particles above 1.2 micron show a relatively flat spectra, while oscillations seem to characterize the medium particles between 0.5 and 1 micron, particles smaller than 0.5 micron are characterized by a spectral slope. These features are illustrated in Figure 2.
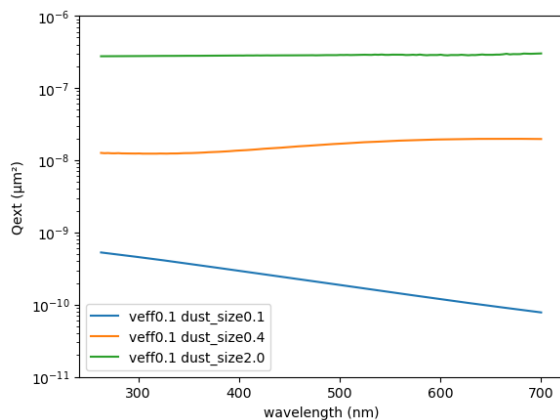

Figure 2 : Example of particles size effect on spectra

Because we are not sensitive to particles with size larger than 1.2 micron. When the fit gives us a value

superior at 1.2, we attribute a value of effective radius (R_{eff}) of 1.5 μm and a standard deviation (V_{eff}) of 0.2 as this is the most common mode observed (Fedorova et al., 2014; Wolff, 2003).
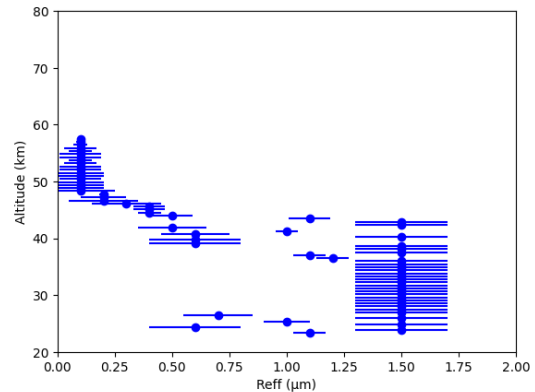

Figure 3: Typical dust size vertical profile

Figure 3 shows an example of retrieved particle size vertical profile. For this example, at low altitude and up to 40km large particle are observed (R_{eff} >1.2 micron). Above 40 km, a decrease in size, in agreement with the expected behavior of size decreasing with altitude is observed.

Dust in the Martian atmosphere is sensitive to seasonal variations. During perihelion (LS 250), the atmosphere of Mars becomes warmer, and dust can be transported to higher altitudes. In the contrary, at the aphelion (LS 70) dust remains confined at lower altitudes.
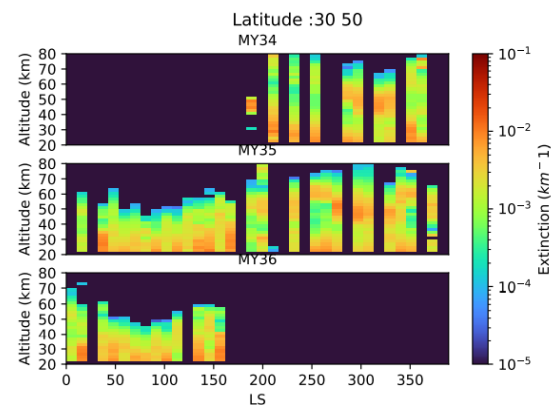
This seasonal variability is shown in Figure 4

Figure 4: Dust vertical extinction profiles versus solar longitude for Mars year 34 to 36

We can see on Figure 4 that at the perihelion dust is present at higher altitudes and the extinction is stronger than during the aphelion. In this work we will further compare the vertical distribution of dust for Mars year 34 (with global dust storm) and Mars year 35 (without global dust strom), as well as latitudinal variations.
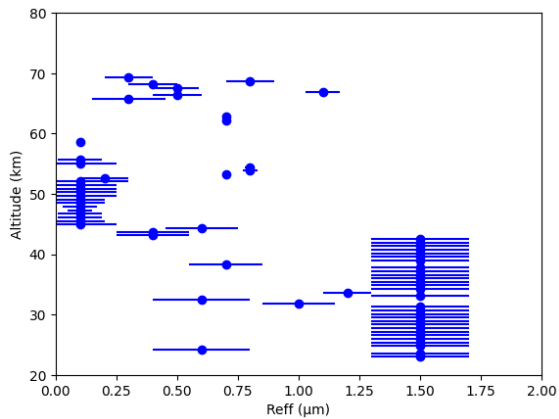
Special case: detection of clouds

Figure 5: Detection of a cloud at high altitude

This characterization of size also helps to detect ice clouds in the atmosphere. A cloud has been detected for example in Figure 5 where we observe an increase of the particle size at high altitude around 70 km. Below that, the particles are smaller, the particles larger than 0.5 micron passed our selection criteria and are considered as real detection. To further confirm the presence of the cloud, a comparison is made with temperature profile derived from the NOMAD SO channel (Trompet, L. et al., 2022). This is illustrated in Figure 6.
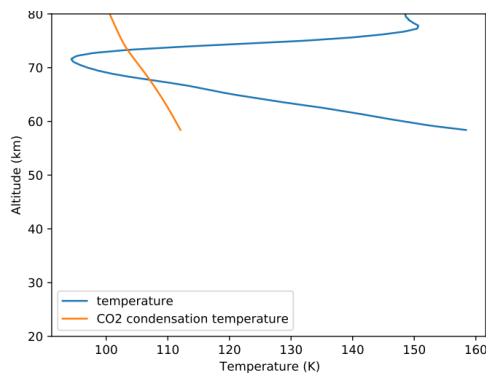
Figure 6 : Comparisons between Temperature profile and CO_2 condensation temperature

We can see that for this particular case the retrieved temperature goes below the CO_2 condensation temperature around 70 km which supports the conclusion of the presence of a CO_2 ice cloud.

References:
Bohren, Craig F. and Donald R. Huffman, Absorption and scattering of light by small particles, New York : Wiley, 1998, 530 p., ISBN 0-471-29340-7, ISBN 978-0-471-29340-8 (second edition)

Clancy, R.T., Grossman, A.W., Wolff, M.J., James, P.B., Rudy, D.J., Billawala, Y.N., Sandor, B.J., Lee, S.W., Muhleman, D.O., 1996. Water Vapor Saturation at Low Altitudes around Mars Aphelion: A Key to Mars Climate? Icarus 122, 36–62. https://doi.org/10.1006/icar.1996.0108

Clancy, R.T., Wolff, M.J., Smith, M.D., Kleinböhl, A., Cantor, B.A., Murchie, S.L., Toigo, A.D., Seelos, K., Lefèvre, F., Montmessin, F., Daerden, F., Sandor, B.J., 2019. The distribution, composition, and particle properties of Mars mesospheric aerosols: An analysis of CRISM visible/near-IR limb spectra with context from near-coincident MCS and MARCI observations. Icarus 328, 246–273. https://doi.org/10.1016/j.icarus.2019.03.025

Fedorova, A.A., Montmessin, F., Rodin, A.V., Korablev, O.I., Määttänen, A., Maltagliati, L., Bertaux, J.-L., 2014. Evidence for a bimodal size distribution for the suspended aerosol particles on Mars. Icarus 231, 239–260. https://doi.org/10.1016/j.icarus.2013.12.015

Holmes, J.A., Lewis, S.R., Patel, M.R., Chaffin, M.S., Cangi, E.M., Deighan, J., Schneider, N.M., Aoki, S., Fedorova, A.A., Kass, D.M., Vandaele, A.C., 2021. Enhanced water loss from the martian atmosphere during a regional-scale dust storm and implications for long-term water loss. Earth Planet. Sci. Lett. 571, 117109. https://doi.org/10.1016/j.epsl.2021.117109

Liuzzi, G., Villanueva, G.L., Trompet, L., Crismani,

M.M.J., Piccialli, A., Aoki, S., Lopez- Valverde, M.A., Stolzenbach, A., Daerden, F., Neary, L., Smith, M.D., Patel, M.R., Lewis, S.R., Clancy, R.T., Thomas, I.R., Ristic, B., Bellucci, G., Lopez- Moreno, J., Vandaele, A.C., 2021. First Detection and Thermal Characterization of Terminator CO_2 Ice Clouds With ExoMars/NOMAD. Geophys. Res. Lett. 48. https://doi.org/10.1029/2021GL095895

Määttänen, A., Listowski, C., Montmessin, F., Maltagliati, L., Reberac, A., Joly, L., Bertaux, J.-L., 2013. A complete climatology of the aerosol vertical distribution on Mars from MEx/SPICAM UV solar occultations. Icarus 223, 892–941. https://doi.org/10.1016/j.icarus.2012.12.001

Montmessin, F., Bertaux, J.-L., Quémerais, E., Korablev, O., Rannou, P., Forget, F., Perrier, S., Fussen, D., Lebonnois, S., Rébérac, A., Dimarellis, E., 2006. Subvisible CO2 ice clouds detected in the mesosphere of Mars. Icarus 183, 403–410. https://doi.org/10.1016/j.icarus.2006.03.015

Trompet, L., Vandaele, A. C., Thomas, I., Aoki, S., Daerden, F., Erwin, J., Flimon, Z., Mahieux, A., Neary, L., Robert, S., Villanueva, G., Liuzzi, G., Lopez-Valverde, M. A., Brines, A., Bellucci, G., Lopez-Moreno, J. J., & Patel, M. R. (2022). Carbon dioxide retrievals from NOMAD-SO on ESA's ExoMars Trace Gas Orbiter and temperature profiles retrievals with the hydrostatic equilibrium equation. I. Description of the method. *Journal of Geophysical Research: Planets, Submitted*.

Vandaele, A.C., Kruglanski, M., Mazière, M.D., n.d. MODELING AND RETRIEVAL OF ATMOSPHERIC SPECTRA USING ASIMUT 6.

Vandaele, A.C., Willame, Y., Depiesse, C., Thomas, I.R., Robert, S., Bolsée, D., Patel, M.R., Mason, J.P., Leese, M., Lesschaeve, S., Antoine, P., Daerden, F., Delanoye, S., Drummond, R., Neefs, E., Ristic, B., Lopez-Moreno, J.-J., Bellucci, G., Nomad Team, 2015. Optical and radiometric models of the NOMAD instrument part I: the UVIS channel. Opt. Express 23, 30028. https://doi.org/10.1364/OE.23.030028

Wilquet, V., Drummond, R., Mahieux, A., Robert, S., Vandaele, A.C., Bertaux, J.-L., 2012. Optical extinction due to aerosols in the upper haze of Venus: Four years of SOIR/VEX observations from 2006 to 2010. Icarus 217, 875–881. https://doi.org/10.1016/j.icarus.2011.11.002

Wolff, M.J., 2003. Constraints on the size of Martian aerosols from Thermal Emission Spectrometer observations. J. Geophys. Res. 108, 5097. https://doi.org/10.1029/2003JE002057

Wolff, M.J., Smith, M.D., Clancy, R.T., Arvidson, R., Seelos, F., Murchie, S., Savijärvi, H., 2009. Wavelength dependence of dust aerosol single scattering albedo as observed by the Compact Reconnaissance Imaging Spectrometer. J. Geophys. Res. 114, E00D04. https://doi.org/10.1029/2009JE003350